THREE DIMENSIONAL FINITE ELEMENT SIMULATION OF COLD FLAT ROLLING

Dr. Abdul Kareem Flaih Hassan   **Hassanein Ibraheem Khalaf**
Mechanical Engineering Department
College of Engineering
University of Basrah
Basrah / Iraq

ABSTRACT

In this paper the finite element analysis of the cold flat rolling is well presented to predict the roll force, slab velocity at entry and exit, temperature rise in the slab during cold rolling, strain and stress distribution around the slab. The effects of friction coefficient and yield stress of slab material on rolling are assumed. It is found that maximum force occurs at the position of neutral point between entry and exit, also it is found that the velocity of slab at exit is larger than that at entry. The finite element results of temperature distribution around the slab predict that there is a considerable rise in slab temperature.

Keywords: Flat Rolling, Finite Element Analysis, Slab, Cold Rolling, Temperature

تمثيل ثلاثي الإبعاد لعملية الدرفلة على البارد باستخدام طريقة العناصر المحددة

أستاذ مساعد دكتور عبد الكريم فليح حسن   **مدرس مساعد حسنين ابراهيم خلف**

قسم الهندسة الميكانيكية

كلية الهندسة   جامعة البصرة

الملخص

في هذا البحث تم تحليل عملية الدرفلة على البارد باستخدام طريقة العناصر المحددة وذلك لغـرض تخمـين القـوة المؤثرة على الدرفيل، سرعة الكتلة المدرفلة في بداية الدخول والخروج من الدرافيل، الارتفاع في درجة حرارة الكتلة نتيجـة التشوه الدن، واخيراً توزيع الانفعال والاجهاد المؤثرة خلال عملية الدرفلة. تم الأخذ بنظر الاعتبار معامل الاحتكـاك واجهـاد الخضوع للمادة المدرفلة. النتائج المستحصلة توضح ان أقصى قيمة للقوة المؤثرة على الدرافيل تكون في نقطة التعادل والتـي تقع في مكان ما على سطح التماس بين منطقة الدخول والخروج كذلك توضح النتائج ان سرعة الكتلة المدرفلة تكون اكبر فـي

منطقة الخروج عن تلك السرعة في منطقة الدخول. ان النتائج المستحصلة بطريقة العناصر المحددة توضح ان هناك ارتفاع في درجة حرارة الكتلة المدرفلة يجب ان تؤخذ بنظر الاعتبار.

INTRODUCTION

Modeling of flat rolling is of great interest to industry due to the large tonnage of such materials consumed and the required quality each year. Modern set-up and control algorithms for rolling mills rely on robust and accurate mathematical models of the roll bite which can predict key parameters such as rolling force, torque and forward slip as a function of the rolling parameters [Jiang, Tieu & Lu, 2004]. The finite element technique has been used as a powerful tool in the modeling of metal forming and found a wide application in this area, in particular, in the flat rolling of steel and aluminum industries. The flat rolling process includes a large deformation, and in general, the elastic deformation is too small to be considered. The plastic deformation, therefore, is the main part that forms the desired shape and products. A rigid-plastic/visco-plastic finite element method has been employed to solve many metal rolling processes, such as flat rolling [Kobayashi, Oh & Altan, 1989], shape rolling [(Mori & Osakada, 1982), (Liu, 1994), (Xiong, Liu & Wang, 2000)], edge-rolling [(Xiong, Liu & Wang, 2000),(Huisman, Huetink, 1985)], special shape steel rolling [(Huisman, Huetink, 1985)] and so on. There are also some issues about the algorithms used to improve the simulation processes [(Jiang, Xiong, Liu, Wang, 1998), (Jiang, Xiong, Liu, Liu, Wang, 2000)]. Moreover, the friction variation [(Jiang, Hu, Thomson, Lam, 2000), (Zhao, Wang, 1987), (Lenard, 1992)] at the strip–roll interface in the deformation zone has an important influence on the simulation results. In flat rolling of slabs, the deformation is inhomogeneous and has a marked effect on the contact stress distribution, the force required to deform the material and residual stresses in the final product, all of which evolve in a way that departs markedly from that under homogenous deformation conditions. Their variation has a crucial effect on the service characteristics and integrity of the finished product [(Vallellano, Cabanillas, Garcˊıa-Lomas, 2008)].

THERORY OF FLAT ROLLING

In rolling processes, the workpiece is rolled between two rolls [**Fig.(1)**], so that the plate is compressed in its thickness direction. As a consequence of this, the plate thickness is reduced. Because of the constancy of volume, the plate must, however, expand in the other directions: in the length direction and also to some extent in the width direction. Rolling can be divided into two types, depending on whether a flat product is rolled, or a product of more complex cross sectional shape is worked. When flat products are rolled, the process is commonly termed flat rolling. In **Fig.(2)**, a slab in rolling process is shown where the initial cross-sectional area A_0 is reduced to A_1. Concurrently, also the initial cross-sectional dimensions of the slab – the thickness H_0 and width B_0 – are changed to H_1 and B_1 after rolling. For this case the length strain can be computed by the following equation [Henry S. Valberg, 2010]:

$$e_x = \ln \frac{l_1}{l_0} = \ln \frac{V/A_1}{V/A_0} = \ln \frac{A_0}{A_1} \tag{1}$$

Another measure of the total deformation is the degree of reduction, specified as the relative area reduction quantified by the expression

$$r(\%) = \frac{A_0 - A_1}{A_0} * 100\% \qquad (2)$$

Transformation from length strain to area reduction, or vice versa, is done by use of the equation:

$$r = 1 - e^{-e_x}$$
(3)

Roll Force Calculation

It is of great importance in industry to be able to predict the required roll force in a rolling operation with acceptable accuracy. In the technical literature, a large number of roll force equations have therefore been proposed. The rolling load in flat rolling, under plane strain conditions, can be expressed by the following formula [Henry S. Valberg, 2010], see **Fig. (3).**

$$F = \frac{2\bar{s}}{\sqrt{3}}\left(1 + \frac{ml}{2(h_0 + h_1)}\right)lB \qquad (4)$$

Workpiece Velocities at Entry and Exit Zone

According to Xincai Tan et.al model [(Xincai, Xiu, Neal, Srinivasan, Jian, 2008)], (for details of this model see Appendix A) the material velocity in the x direction is then given by

$$V_x = \frac{h_o V_0}{2z} = \frac{h_1 V_1}{2z} \qquad (5)$$

IMPLEMENTATION

The finite element package ***DEFORM-3D*** version 6.1 was used to simulate the process of cold flat rolling as follows:

Material Data and Geometry

An Aluminum slab of Al6061 with dimensions 100x30x500 mm (wxhx*l*) was used as a the slab material in this simulation, see **Fig.(4-a),** while the roll material was assumed to be rigid. The roll diameter, roll width was 300, 200mm respectively, **Fig.(4-b).** The gap between the two rolls was 22mm, roll speed was 12 rpm and the rolling operation achieved in one pass ($\Delta h=30-22= 8mm$)under temperature of 20 ºC. A full 3D model is shown in **Fig.(4-c).**

Finite Element Mesh

The finite element mesh used in this simulation for a full model of the slab is shown in **Fig.(5).** The type of element is brick element with total number of element of 4536 and total number of nodes of 5698 nodes.

VALIDATION OF THE SIMULATION MODEL

To validate the above model, it is necessary to compare the predicted results obtained by the finite element package ***DEFORM-3D*** with other results predicted by analytical models.

Roll Force and Roll Torque

The roll force per unit width *F* can be calculated using the analytical formula of Hitchcock's [(Gudur, Salunkhe, Dixit, 2008)].

$$F = \int_0^L \left(P + \frac{x}{R} t \right) dx \tag{6}$$

Where *P* is the normal contact pressure, L is the projected contact length, *x* is the distance from the roll centre, R is the roll radius, and τ is the frictional shear stress at the interfaces.

The roll force and torque calculated by the ***DEFORM-3D*** FE package are shown in **Fig.(6).** The maximum load predicted by the finite element simulation has been observed at the neutral point with a value of 2.57 MN, while the roll force estimated using Hitchcock's formula gives a prediction of 2.53 MN, see appendix A which is found in a good agreement (Maximum percentage error of 2%) with the results of FE prediction.

Velocity at Entry and Exit Zone

Table(1) shows a comparison between the result of FE simulation and the analytical result of Ref.[(Xincai, Xiu, Neal, Srinivasan, Jian, 2008)], see appendix A. It seems that both resuls are in good agreemnt with a maximum percentage error of 13%. **Fig.(7)** shows the countor plot of the velocities at entry and exit for the simulated results of the finite elemnt model.

RESULTS AND DISCUSSION

Distribution of Effective Strain and Stress

Figs. (8) and (9) show the contour plot of the effective strain and stress, around the work piece, respectively during the rolling process. It can be seen that the maximum value of effective strain is 0.53 and will be reached after 0.3644 sec. of process time, while a maximum value of 486 MPa effective stresses was reached after 0.2186 sec.

Temperature Evolution during Cold Bar Rolling

The temperature rise of the workpiece during cold rolling can be attributed to various factors such as rolling speed, initial temperature of the billet, plastic deformation of the workpiece, the cross sectional shape of the workpiece at each pass, cooling condition in the individual passes. As known above the rolling process achieved at temperature 20C, **Fig,(10)** illustrates the temperature distribution around the workpiece with maximum value 109 C.

CONCLUSIONS

The following conclusions may be achieved from the results presented in this paper:
1. The results obtained from the present work verify that the process of cold flat rolling could be theoretically estimated using the finite element method with a reasonable degree of accuracy.
2. Roll force and velocity at entry and exit for a specific rolling conditions could be predicted
3. Temperature rise during the cold flat rolling for known conditions could be estimated.

REFERENCES

C. Vallellano , P.A. Cabanillas, F.J. Garc´ıa-Lomas,"Analysis of deformations and stresses in flat rolling of wire", journal of materials processing technology 1 9 5 (2 0 0 8) 63–71.

H.J. Huisman, J. Huetink, "Combined Eulerian Lagrangian three dimensional finite-element analysis of edge-rolling", J. Mech. Working Technol. 21 (1985) 333–353.

Henry S. Valberg , "Apllied Metal Forming Including FEM Analysis" Published in the United States of America by Cambridge University Press, New York, 2010.

J.G. Lenard, "Friction and forward slip in cold strip rolling", Tribology. Trans. 35 (3) (1992) 423–428.

K. Mori, K. Osakada, "Simulation of three-dimensional rolling by the rigid-plastic finite element method", Proceedings of the International Conference Numerical Methods in Industrial Forming Processes, Pineridge Press, Swansea, 1982, pp. 747–756.

P.P Gudur, M.A. Salunkhe, U.S. Dixit,"A theoretical study on the application of asymmetrical rolling for the estimation of friction", International Journal of Mechanical Sciences, 50 (2008) 315-327.

S. Kobayashi, S.I. Oh, T. Altan, "Metal Forming and Finite Element Method", Oxford University Press, New York, 1989, pp. 222–243.

S.W. Xiong, X.H. Liu, G.D. Wang, "Analysis of non-steady state slab edging in roughing trains by a three-dimensional rigid-plastic finite element method", Int. J. Mach. Tools Manuf. 40 (11) (2000),1573–1585

X.H. Liu, "Rigid-Plastic FEM and its Application in Steel Rolling", Metallurgy Industrial Press, Beijing, 1994, pp. 235–275.

Xincai Tan, Xiu Tan Yan, Neal P. Juster, Srinivasan Raghunathan, Jian Wang, "Dynamic friction model and its application in flat rolling", Journal of Materials Processing Technology, 207, 2008, 222-234.

Z. Zhao, G.D. Wang, "Modern Plastic Forming Mechanics", Northeastern University Press, Shenyang, 1987, pp. 150–153.

Z.Y. Jiang, S.W. Xiong, X.H. Liu, G.D. Wang, "3D rigid-plastic FEM analysis of the rolling of a strip with local residual deformation", J. Mater. Process. Technol. 79 (1998) 109–112.

Z.Y. Jiang, W.P. Hu, P.F. Thomson, Y.C. Lam, "Solution of the equations of rigid plastic FE analysis by shifted incomplete Cholesky factorisation and the conjugate gradient method in metal forming processes", J. Mater. Process. Technol. 102 (1–3) (2000) 70–77.

Z.Y. Jiang, X.L. Liu, X.H. Liu, G.D. Wang,"Analysis of ribbed-strip rolling by rigid visco-plastic FEM", Int. J. Mech. Sci. 42 (2000) 693–703.

Z.Y. Jiang*, A.K. Tieu, C. Lu,"A FEM modeling of the elastic deformation zones in flat rolling", Journal of Materials Processing Technology ,146 (2004), 167–174.

APPENDIX A

As shown in **Fig.(A1),** the volume rate of material flow due to volume constancy can be written as [(Xincai, Xiu, Neal, Srinivasan, Jian, 2008)]

$$wh_0V_0 = w(2z)V_x = wh_1V_1$$

Where w is the width of the strip, h_0 and h1 are the initial thickness at the entry side and the final thickness at the exit side, respectively; z is half height in the deforming region corresponding to x coordinate; V_0, V_x, and V_1 are the velocities in the x direction corresponding to h_0, z, h_1, respectively. The material velocity in the x direction is then given by

$$V_x = \frac{h_0V_0}{2z} = \frac{h_1V_1}{2z}$$

Where

$$z = z_0 - \sqrt{R_e^2 - X^2}$$

$$X^2 + (Z - Z_0)^2 = R_e^2$$

Z_0 is a constant for a given rolling process, and R_e is the effective radius

$$z_0 = R_e + \frac{h_1}{2}$$

$$R_e = \frac{L_e^2}{\Delta h} + \frac{\Delta h}{4} = R + \Delta R$$

Where R_e is the effective contact length, Δh is the draft during rolling, and ΔR is the difference of the radii between the deformed arc and the nominal arc. An approximate value of ΔR will be estimated for each rolling process during the deformation.

$L_e = (1 + S_f)L_c$ where S_f is forward slip, and L_c is the nominal contact length

$$\Delta h = h_0 - h_1$$

$$\Delta R = L_c^2 (2S_f + S_f^2)/\Delta h$$

$$L_c = \sqrt{R\Delta h - \Delta h^2/4}$$

$$S_f = \frac{L_e}{L_c} - 1$$

From the definition of forward slip,

$S_f = (V_1 - V_R)/V_R$, so V_1 can be given as a function of S_f

$V_1 = V_R(1 + S_f)$ where V_R is the linear velocity of the roll surface.

Table(1): Comparison Between FE Results and Analytical Results of Ref.[16]

Time	Present work results		Analytical results Ref.[16]	
	Entary velocity V_0 (mm/sec)	Exit velocity V_1 (mm/sec)	Entary velocity V_0 (mm/sec)	Exit velocity V_1 (mm/sec)
Step 10	161	183	163	185
Step 20	163	184	165	188
Step 30	165	186	167	190
Step 40	166	187	168	191
Step 60	167	188	170	193
Step 70	178	189	182	192
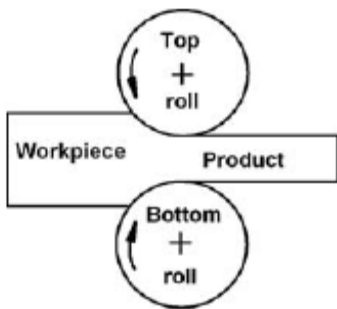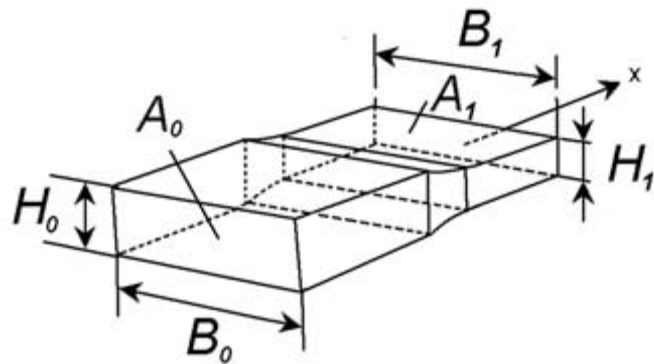
Fig.(1) Flat Rolling   Fig.(2) Workpiece Configurations in Situations Rolling
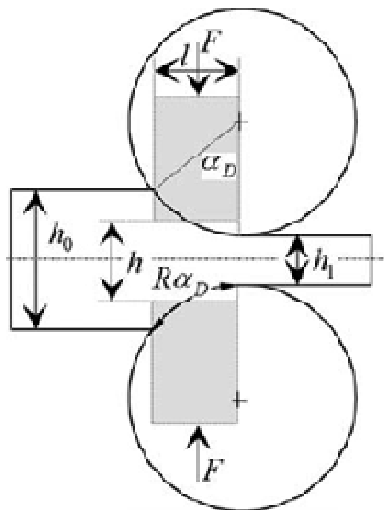
Fig.(3) Rolling Considered as Equivalent to Plane Strain Compression to Deduce a Rolling Load Formula
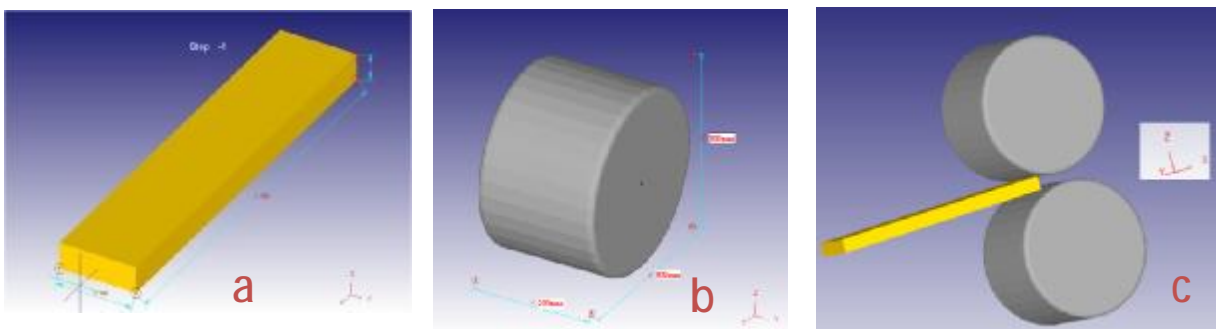
Fig.(4) Geometry of Slab and Roll

(a) Slab Dimensions   (b) Roll Dimensions   (c) 3D Full Model
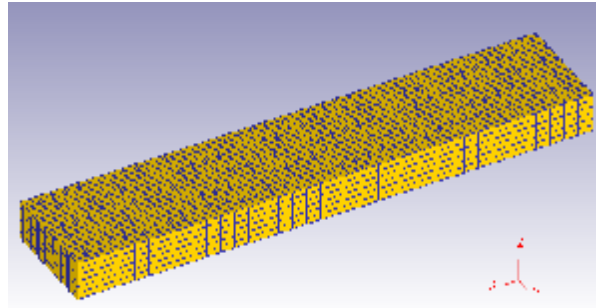
Fig.(5) The Meshed Slab
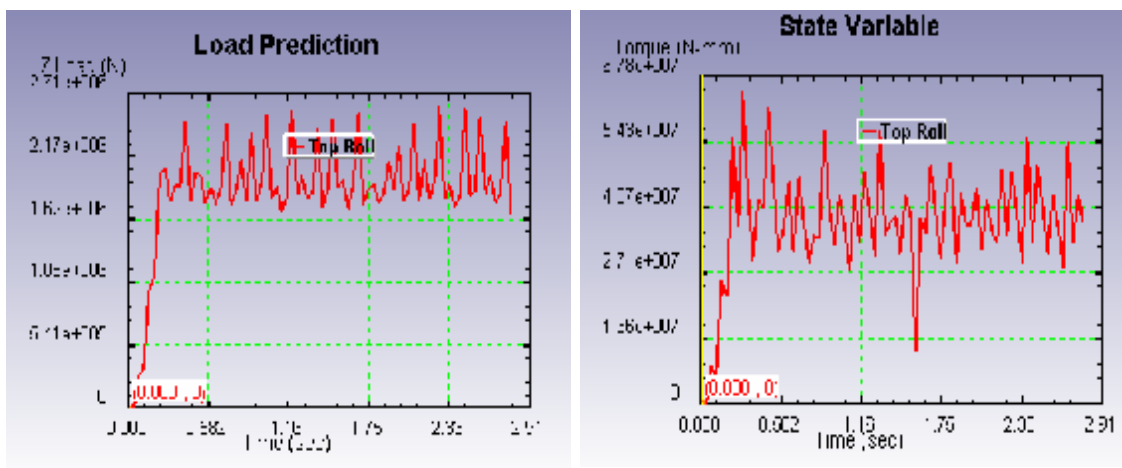
Fig. (6) Variation of Roll Force and Roll Torque During the Rolling Process
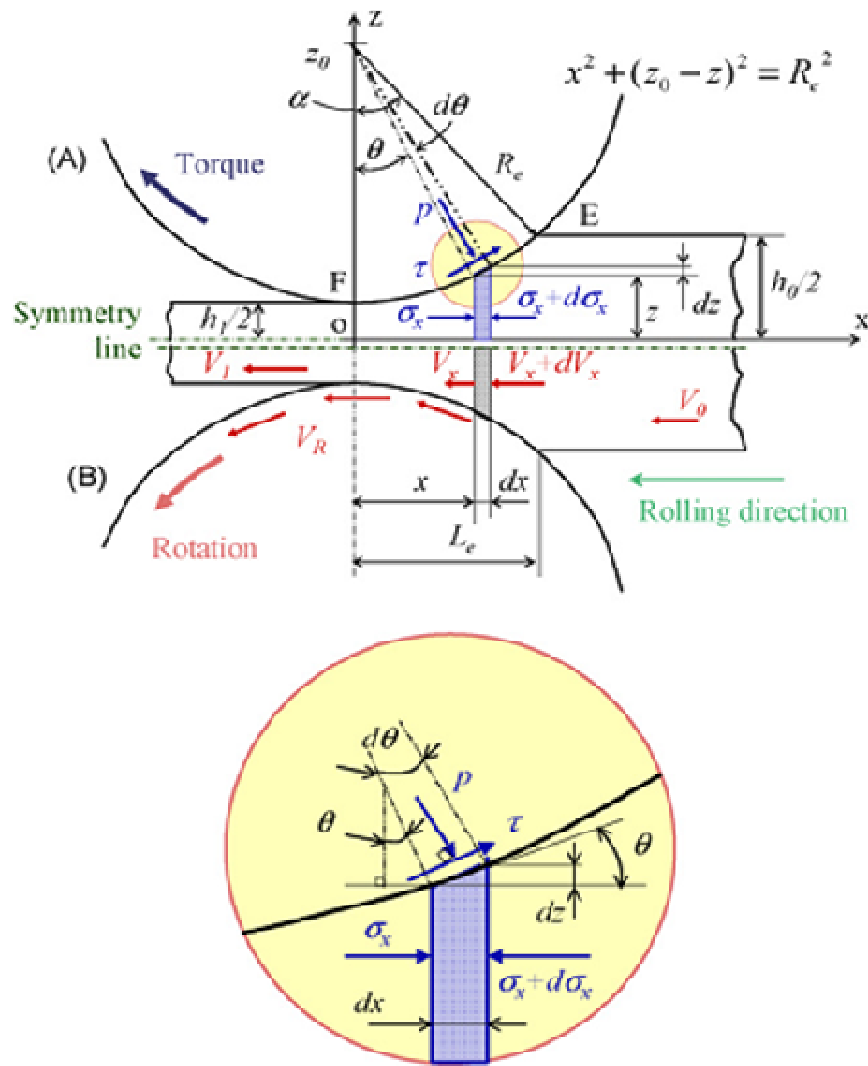
Fig. (A1) Equilibrium of Forces in the Deformation Zone and Various Velocities in the Roll Gap During Flat Rolling
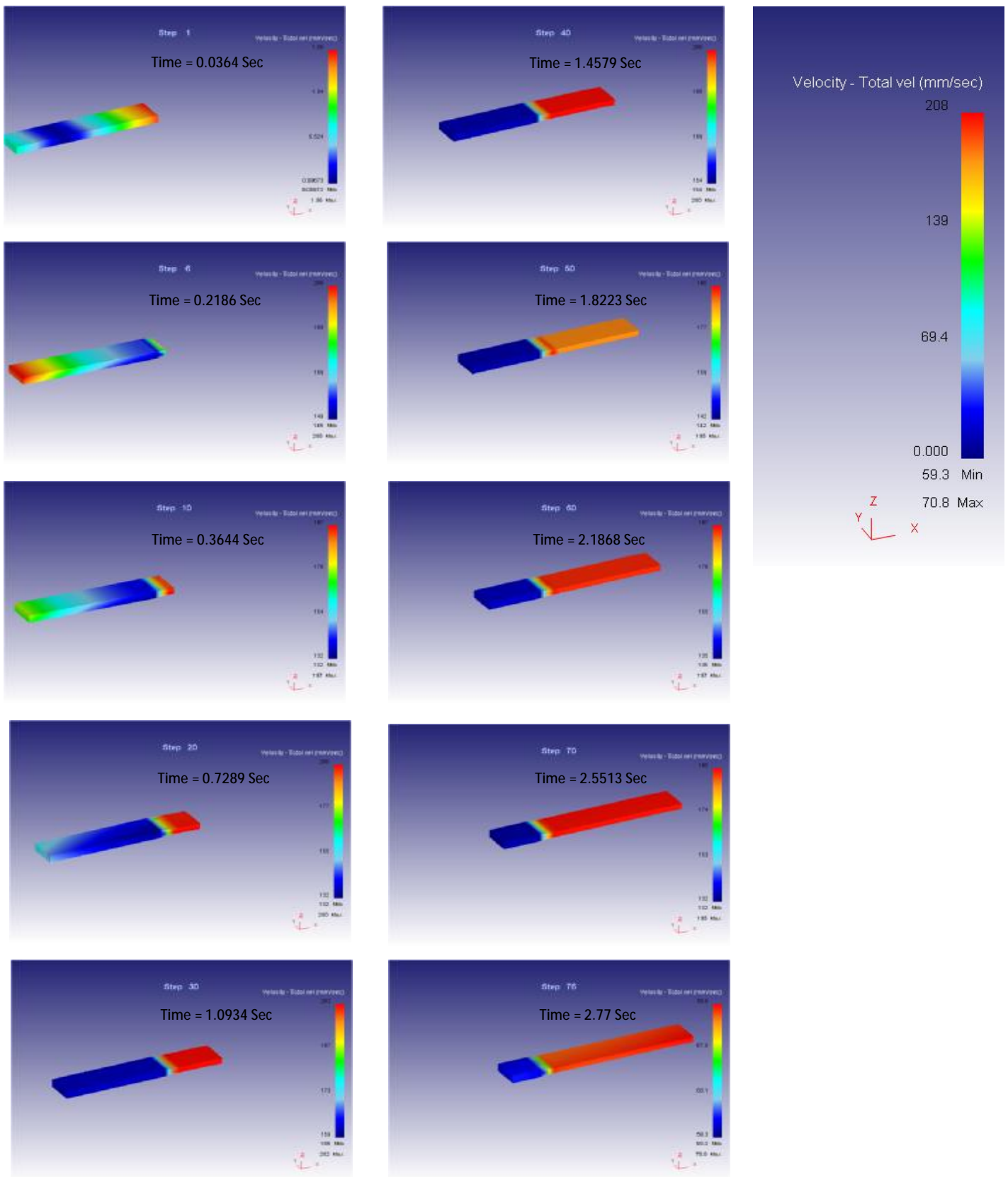
Fig. (7): Counter Plot of Due Velocities During the Rolling Process
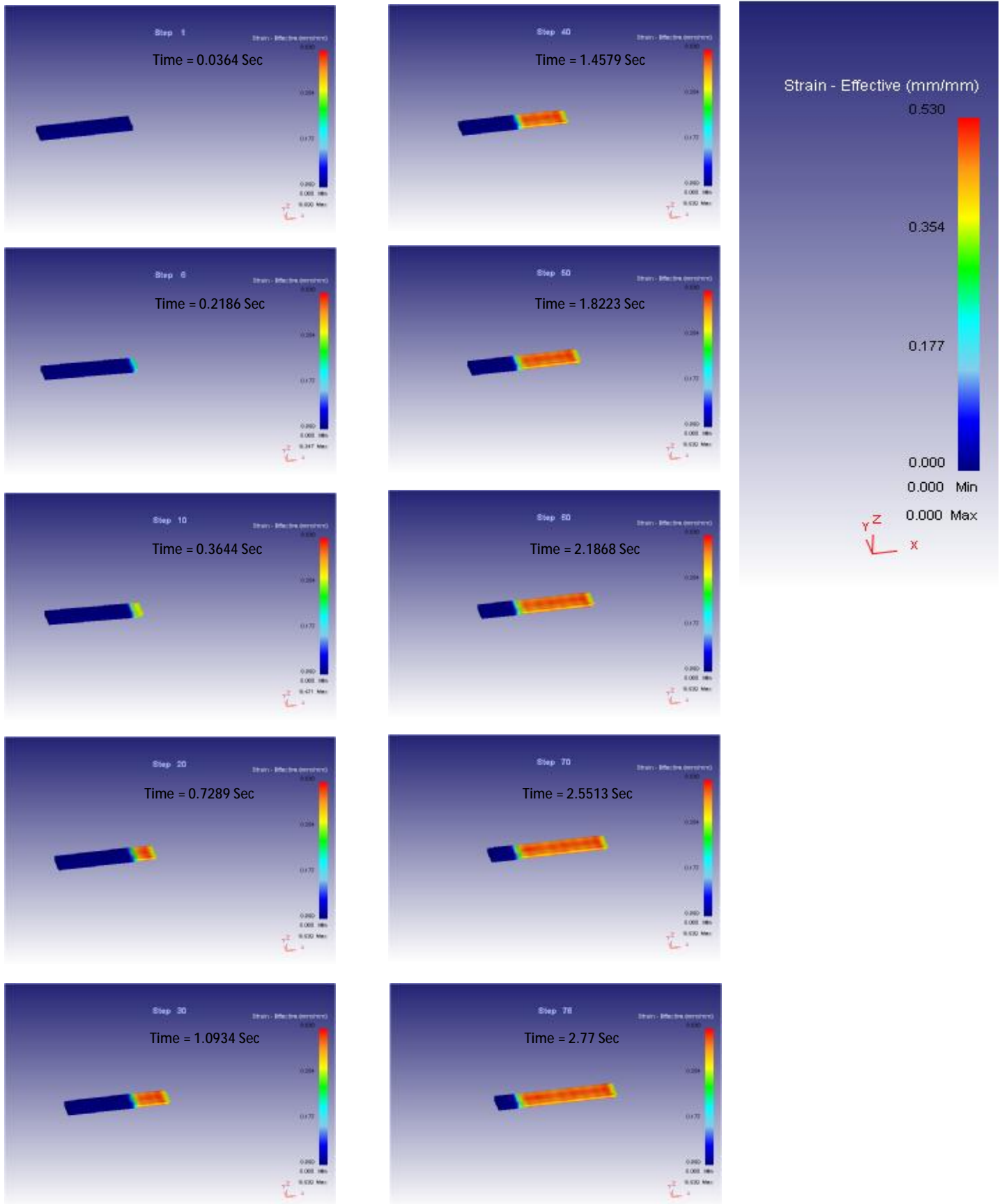
Fig. (8): Distribution of Effective Strain Around the Slab
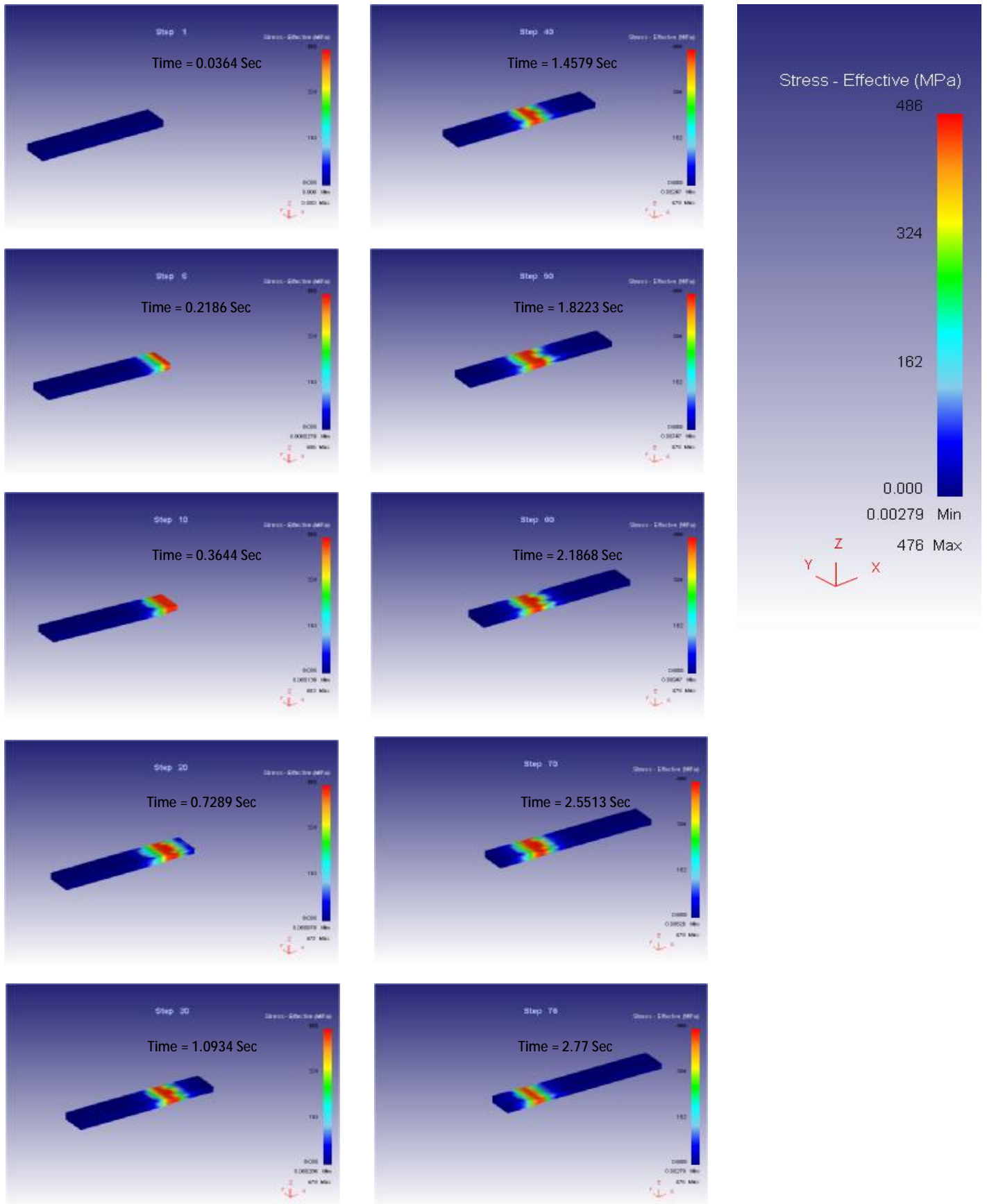
Fig. (9): Distribution of Effective Stress Around the Slab

Fig. (10): Temperature Distribution Around the Slab